INVENTORY OF SUPPLEMENTAL MATERIALS:

Figure S1, Related to Figure 1. Includes details of proximity analysis methodology and comparison to other network methods.

Figure S2, Related to Figures 1 and 2. Presents details of proximity analysis in epidermal differentiation and MPZL3 expression patterns. Supports data shown in Figure 2 with additional details of MPZL3 regulating the induction of epidermal differentiation genes.

Figure S3, Related to Figure 3. Shows that MPZL3 localizes to the mitochondria in fractionation experiments and the mitochondrial phenotypes regulated by MPZL3.

Figure S4, Related to Figure 3. Depicts results of knock down of several MPZL3 interaction partners and details FDXR and mutant MPZL3 expression and localization.

Figure S5, Related to Figure 5. Demonstrates additional details of MPZL3 and FDXR ROS regulation and results of ROS modulation in epidermal differentiation.

Figure S6, Related to Figure 6. Contains additional details of FDXR enzymatic functions and expression and localization of FDXR mutants.

Table S1, Related to Figure 1. Complete network file for *S. cerevisiae* network. Indicates both nodes of an edge as well as the probability of inclusion in the network.

Table S2, Related to Figure 1. Complete network file for epidermal differentiation network. Indicates both nodes of an edge as well as the probability of inclusion in the network.

Table S3, Related to Figure 1. Dynamic hub scores for most connected nodes from proximity analysis.

Table S4, Related to Figure 2. MPZL3 regulated genes with fold change values.

Table S5, Related to Figure 3. Relative levels of metabolites from differentiated keratinocytes treated with either control siRNA or siRNAs against MPZL3.

Table S6, Related to Figure 4. FDXR regulated genes with fold change values.

Supplementary Experimental Procedures

Supplementary References

Supplemental Fig 1. Proximity Analysis With Topological Constraints

A

Rank Order Based Correlation Matrix

Gene	A	B	C	D	X
A	1	c_{ab}	c_{ac}	c_{ad}	c_{ax}
B		1	c_{bc}	c_{bd}	c_{bx}
C			1	c_{cd}	c_{cx}
D				1	c_{dx}
X					1

c_{ij} = proximity value

B

$$P_{ij} = \frac{k_j}{\sum_a k_a} * c_{ij}$$

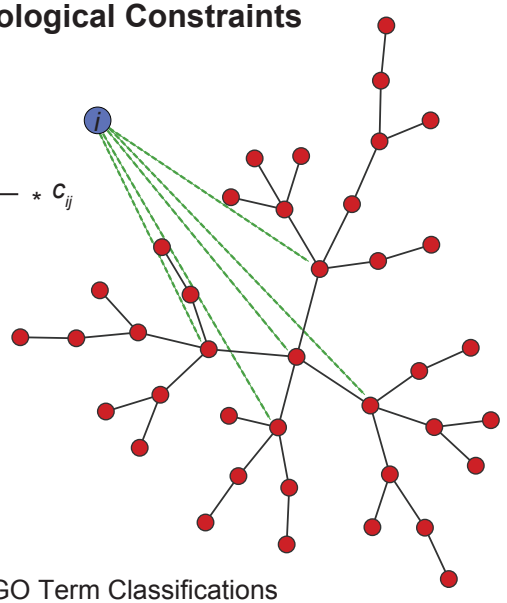

C

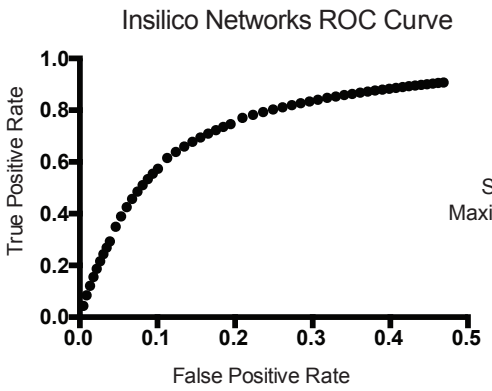

Variables:
Seed Network Size
Seed Network Connectivity
Maximum New Node Connections

D

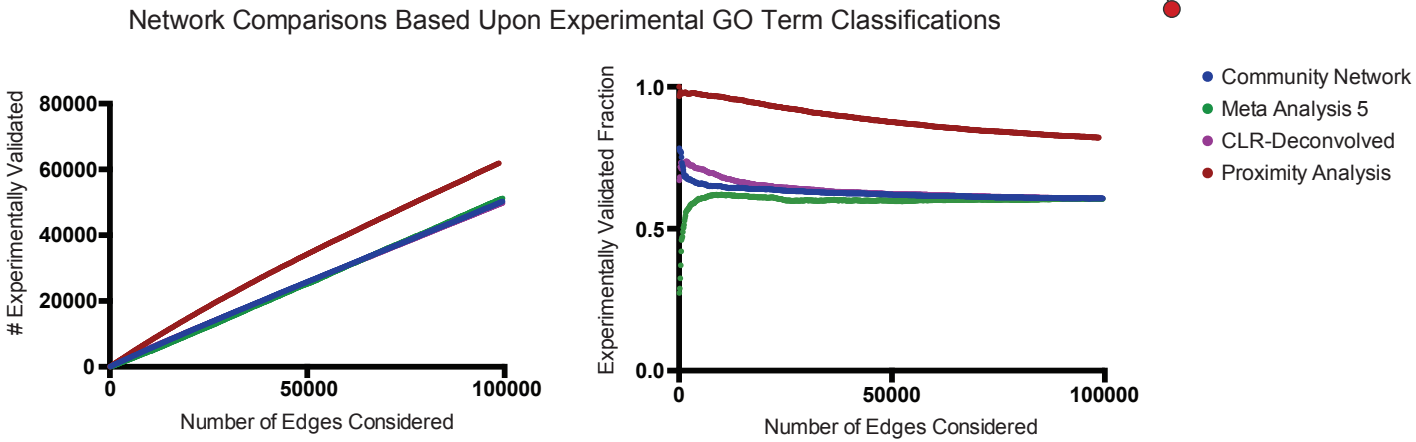

E

Topology Summary

Method	Average Clustering Coefficient	Power Law Degree of Distribution
Community	0.7230	2.34
Meta Analysis 5	0.7341	2.86
CLR Deconvolved	0.6984	2.28
Proximity Analysis	0.7607	2.91

F

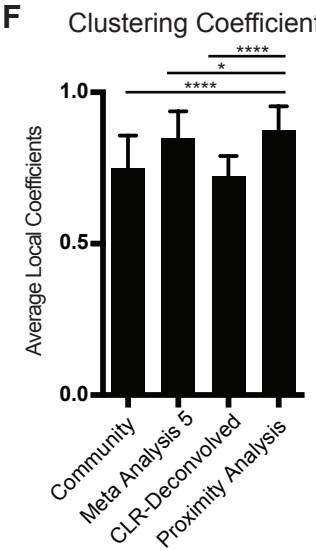

G

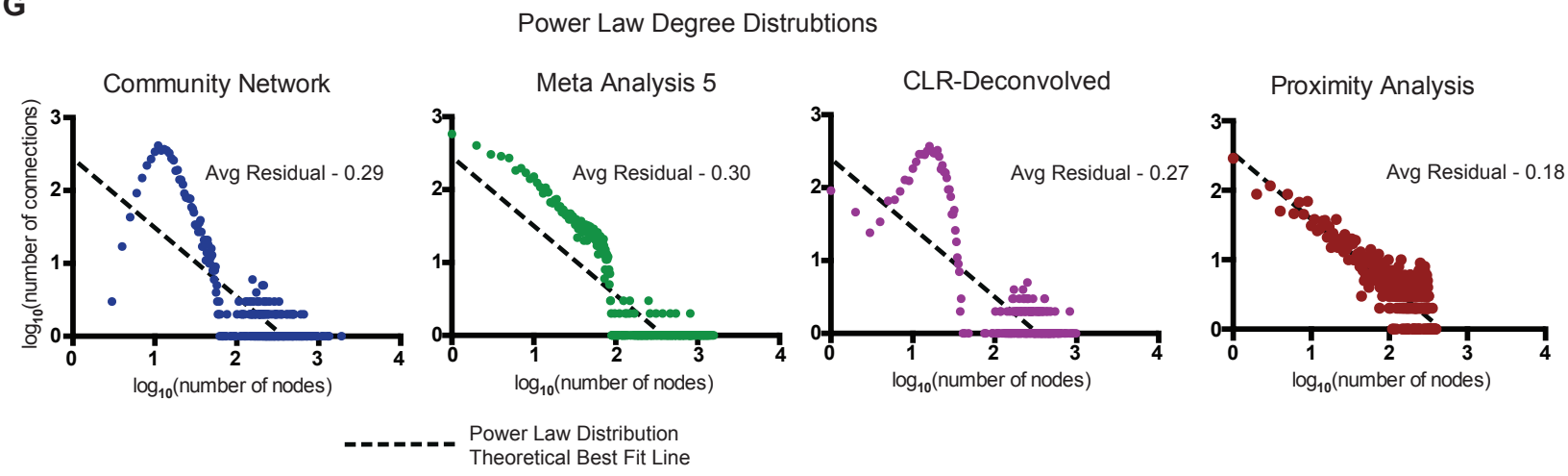

Supplemental Fig 2. Proximity Analysis of Epidermal Differentiation

A Topology Summary

Method	Average Clustering Coefficient	Power Law Degree of Distribution
Proximity Analysis	0.7101	2.57

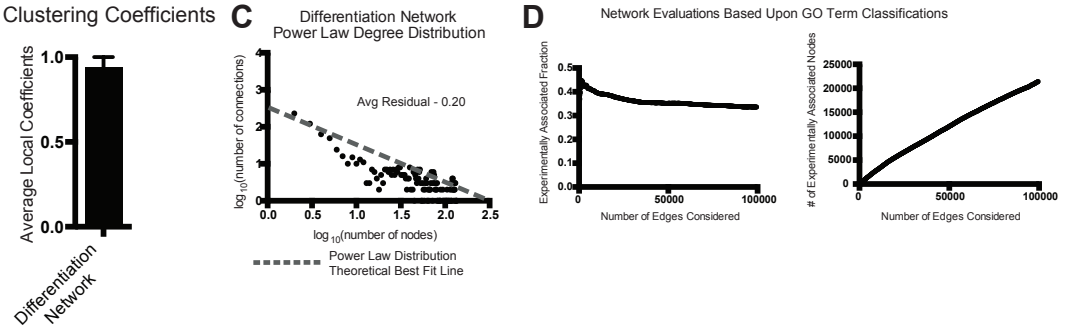

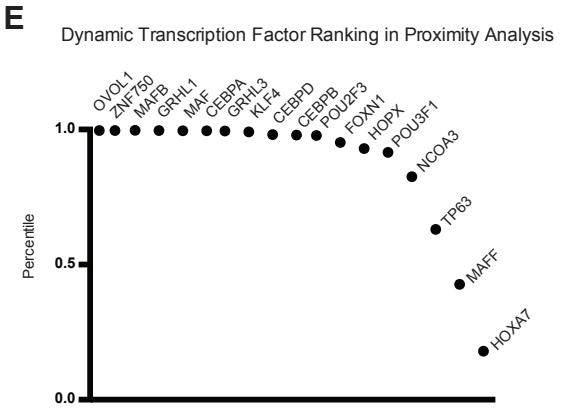

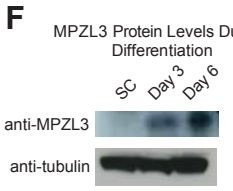

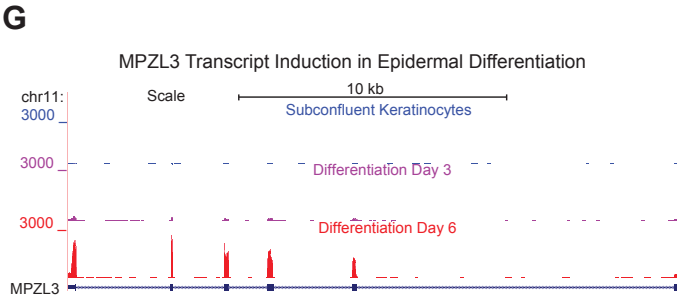

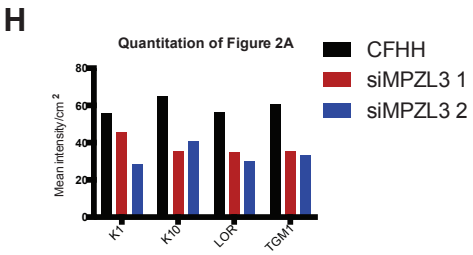

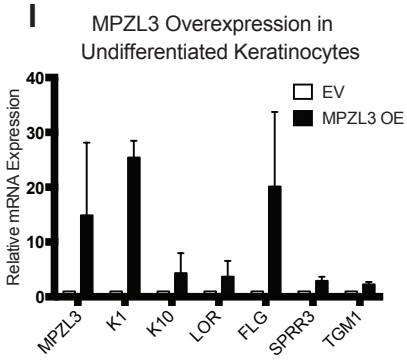

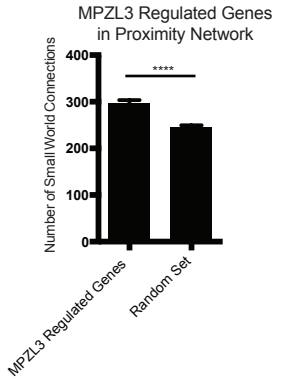

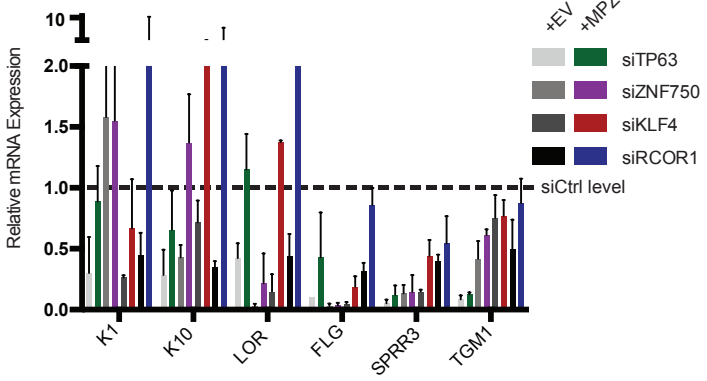

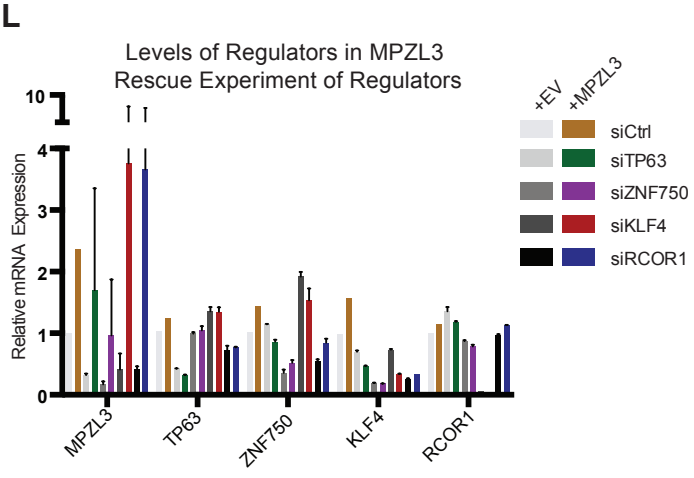

Supplemental Fig 3. MPZL3 in the Mitochondria

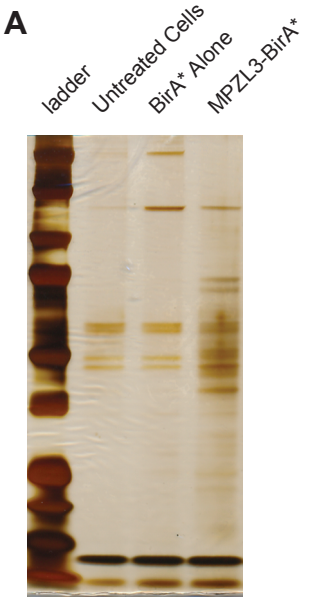

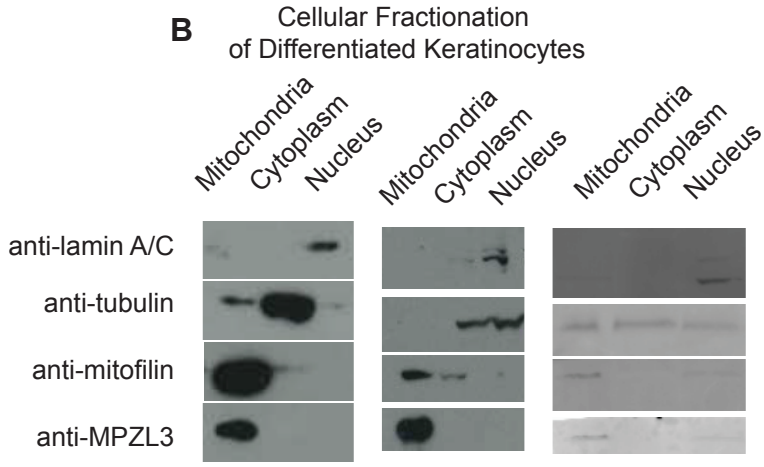

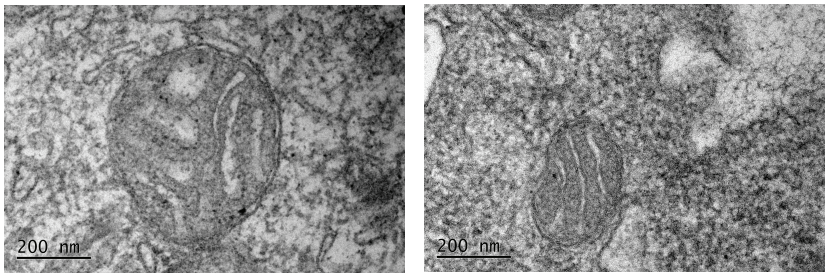

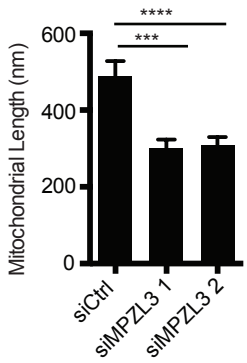

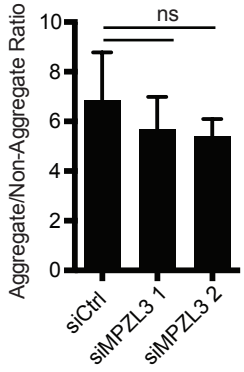

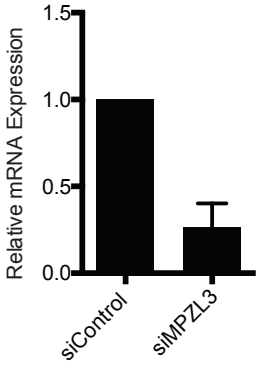

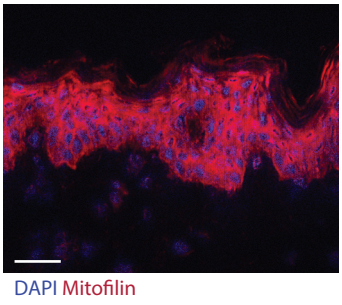

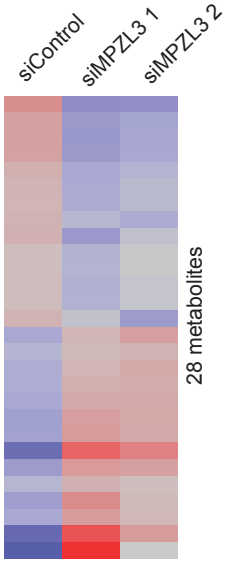

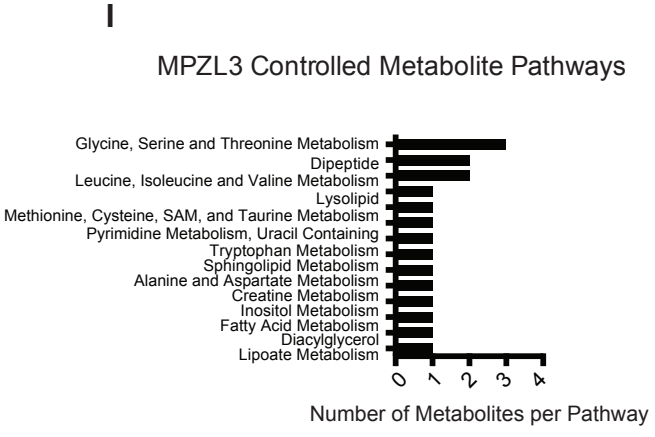

Supplemental Fig 4. MPZL3 and FDXR are Mitochondrial Proteins that Interact

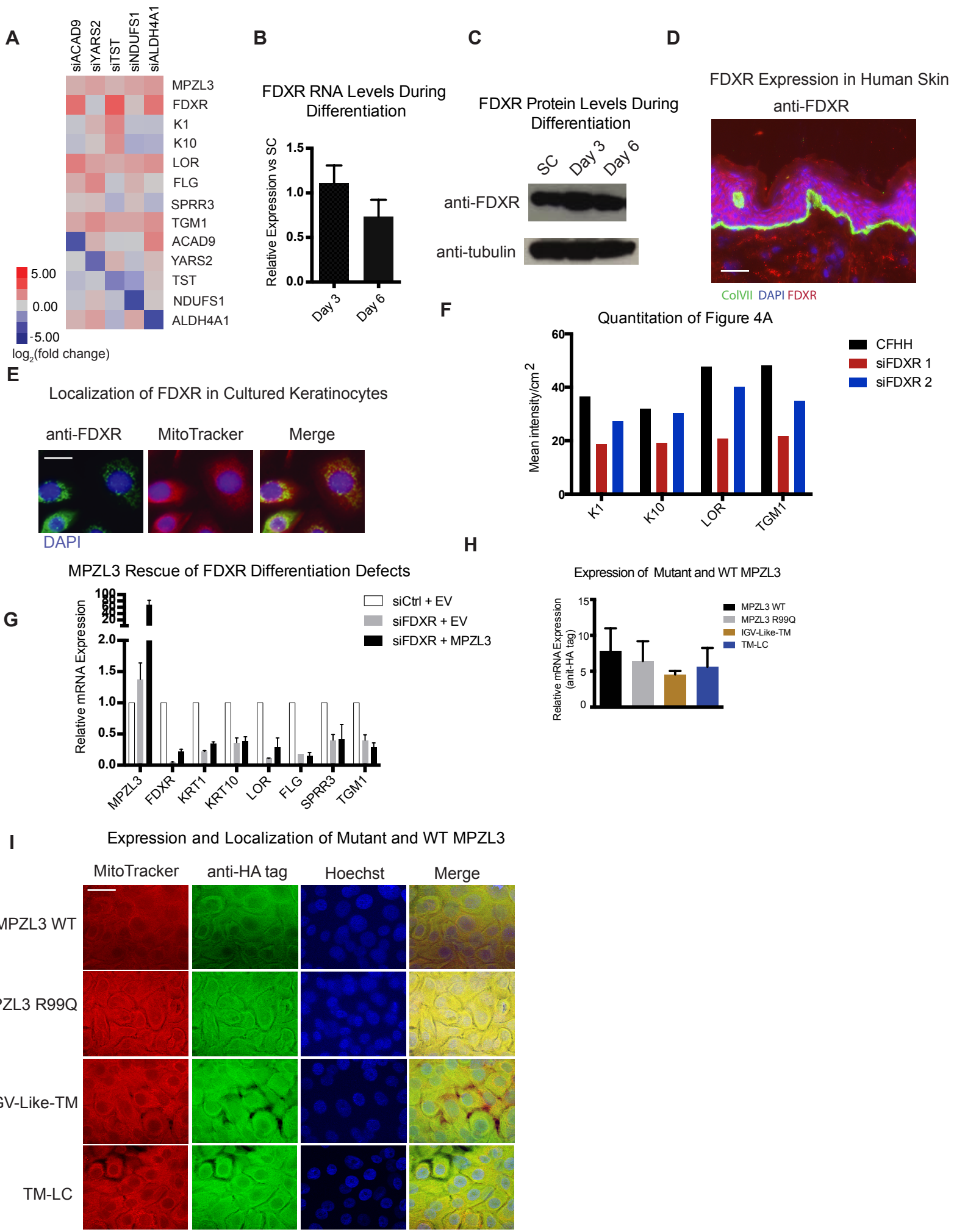

Supplemental Fig 5. MPZL3 and FDXR Regulate ROS

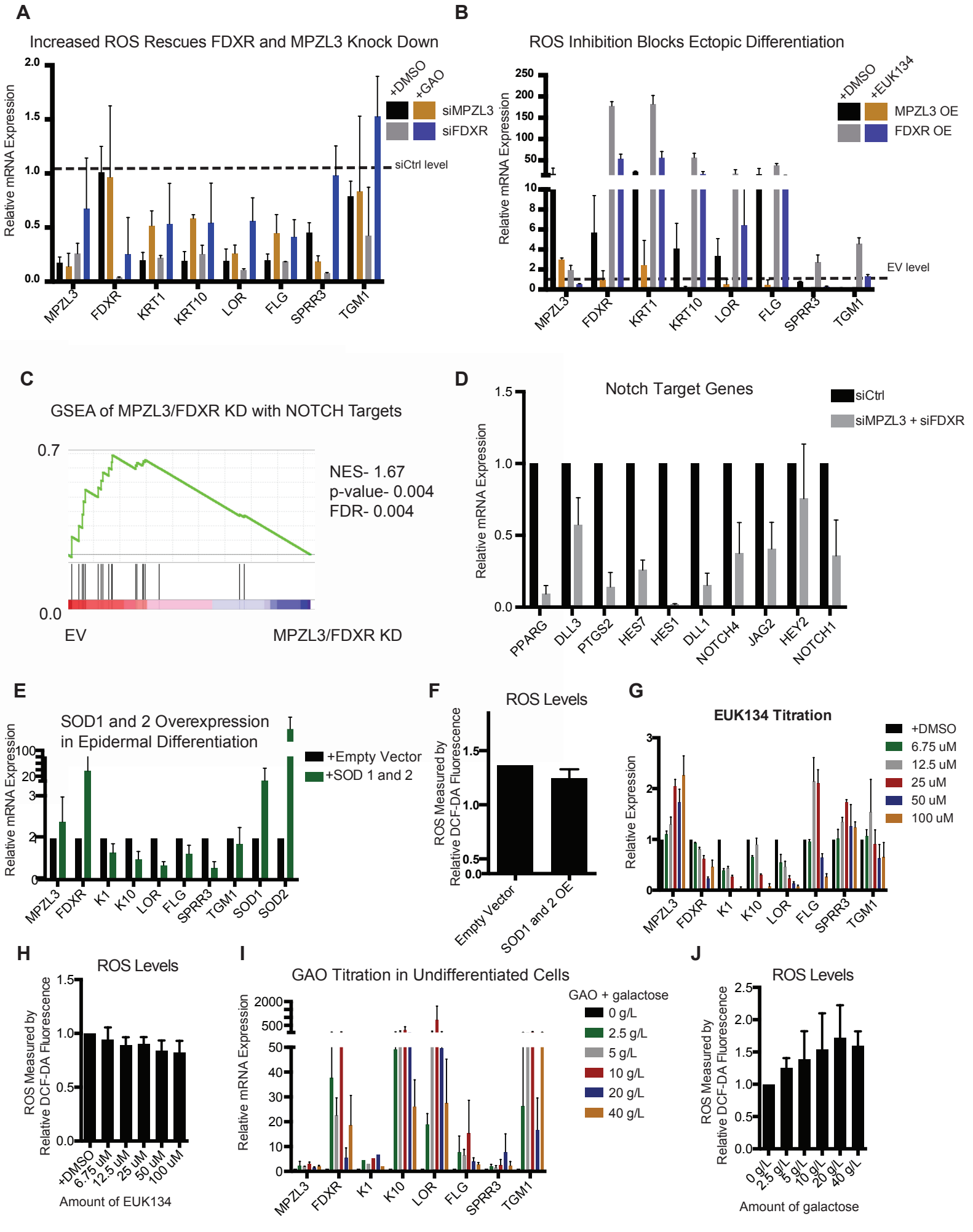

Supplemental Fig 6. FDXR Enzymatic Activity in Differentiation

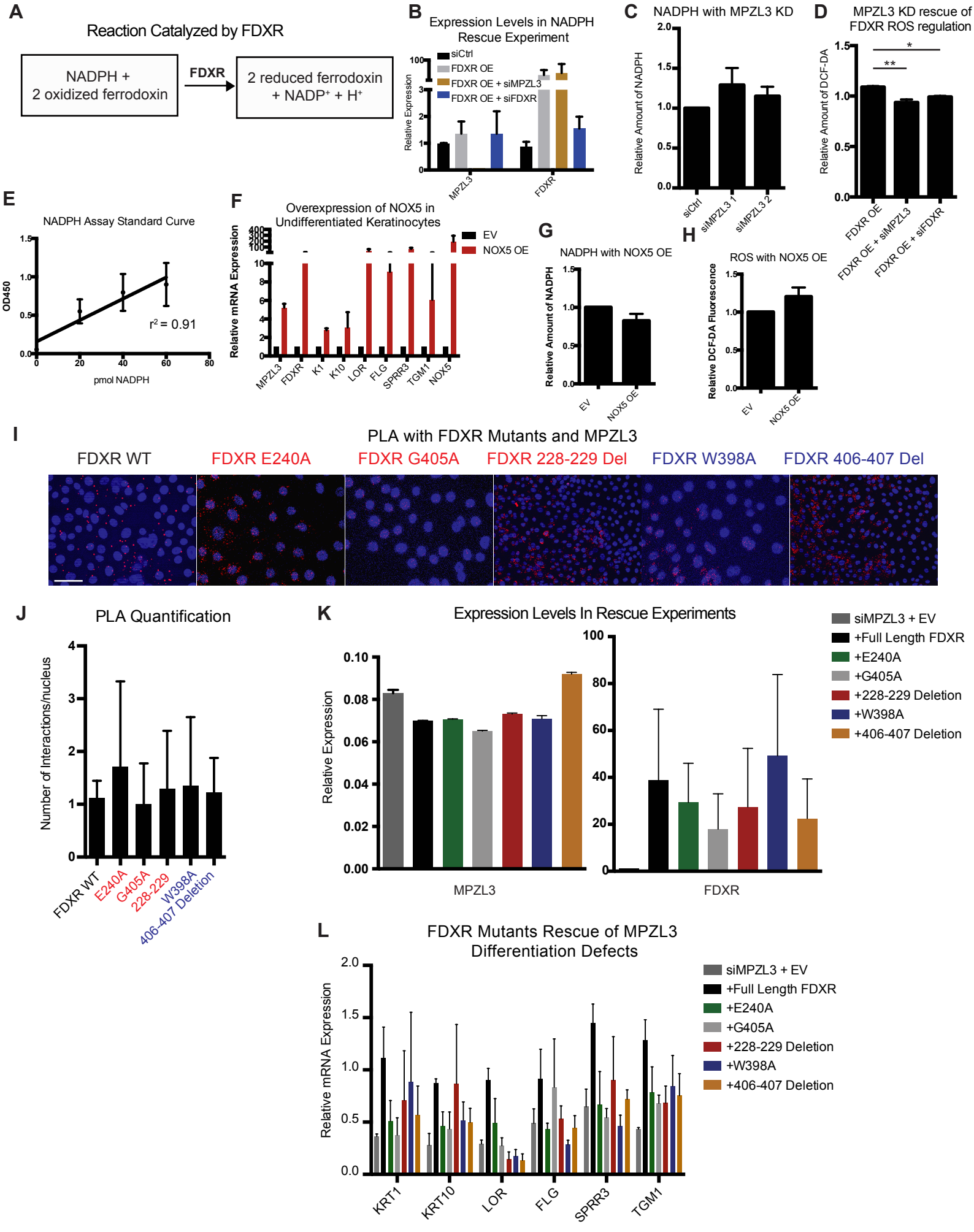

SUPPLEMENTAL FIGURE LEGENDS

Supplemental Figure 1. Proximity Analysis with Topological Constraints (Related to Figure 1) (A) Example matrix representing the rank ordered correlation matrix derived from proximity analysis. **(B)** Model depicting the way that proximity analysis attaches nodes to a seed network, as weighted by the correlation coefficient. **(C)** A Receiver Operator Curve (ROC) depicting the process of *in silico* parameter optimization. The apex of the curve was the combination of parameters chosen for downstream analyses. **(D)** Network comparisons based upon identification of edges with the same GO Term based upon *Saccharomyces Cerevisiae* networks. Other network algorithms results used from previous work: Community, Meta-Analysis (Marbach et al., 2012) or CLR-ND (Feizi et al., 2013). **(E)** Topology summary including clustering coefficients and power law degree of distribution for the networks analyzed in (D). **(F)** Clustering coefficients in proximity analysis are significantly higher than other networks analyzed. Mean +/- SEM shown. **(G)** Node degree distributions for each of the networks analyzed. Proximity analysis has the smallest residual.

Supplemental Figure 2. Proximity Analysis of Epidermal Differentiation (Related to Figures 1 and 2) (A) Topology summary of the network resulting from applying proximity analysis to epidermal differentiation time course data. The network is scale-free and small-world. **(B)** Representation of the average clustering coefficients +/- SEM in the differentiation network. **(C)** Node degree distribution for the epidermal differentiation network. **(D)** Network evaluation based upon the number of edges that belong to the same GO Term in the differentiation network. **(E)** Ranking of transcription factors known to be expressed in epidermal differentiation and/or regulators of the process. **(F)** Western blots showing MPZL3 protein levels in epidermal differentiation. **(G)** RNA-Sequencing tracks showing the transcript level induction of MPZL3 in Day 3 and Day 6 compared to subconfluent, undifferentiated keratinocytes (Kretz et al., 2012). **(H)** Quantification of the signal for differentiation markers in Figure 2A. **(I)** Differentiation marker transcript levels with overexpression of MPZL3 in undifferentiated keratinocytes. **(J)** Number of small world connections for genes regulated by MPZL3 compared to a random set. p-value < 0.0001, mean +/- SEM shown. **(K)** Bar graph detailing the values of the MPZL3 rescue in the context of epidermal regulator depletion. Mean +/- SD shown. **(L)** Levels of the epidermal regulators in the MPZL3 rescue experiment. Mean +/- SD shown.

Supplemental Figure 3. MPZL3 in the Mitochondria (Related to Figure 3) (A) Silver stain showing the levels of protein obtained from either untreated differentiated keratinocytes, BirA* alone, or MPZL3-BirA* fusions. **(B)** Western blots showing a mitochondrial, cytoplasmic, nuclear fractionation of differentiated keratinocytes showing MPZL3 in the mitochondrial fraction. Three independent experiments are presented. **(C)** Electron microscopy of representative images showing the mitochondrial size of differentiated keratinocytes treated with control siRNA or independent siRNAs against MPZL3. **(D)** Quantification of the mitochondrial size shown in (D). **(E)** Quantitation of JC-1 signal interrogating mitochondrial membrane potential in differentiated keratinocytes treated with control siRNA or independent siRNAs against MPZL3. **(F)** Quantification of MPZL3 knockdown in the experiments shown in (D-F) **(G)** Immunofluorescence showing mitofilin, a mitochondrial protein, localizing to all layers of the epidermis excepting the stratum corneum. Bar 15 μM. **(H)** Heatmap showing metabolites changed significantly in at least one sample with an siRNA against MPZL3 as compared to a control siRNA. **(I)** Bar graph showing which pathways metabolites shown in (J) are related to.

Supplemental Figure 4. MPZL3 and FDXR are Mitochondrial Proteins that Interact (Related to Figure 3) (A) Heatmap showing the impact of the knockdown of the top 5 MPZL3 mitochondrial interaction partners **(B)** Transcript levels of FDXR over the course of differentiation as a fold change compared to undifferentiated subconfluent (SC) keratinocytes. **(C)** Western blot showing FDXR protein levels in epidermal differentiation. **(D)** Immunofluorescence of FDXR in human skin. Bar 15 μM. **(E)** Immunofluorescence showing localization FDXR to the mitochondria as labeled by MitoTracker. Bar 3 μM. **(F)** Quantification of the signal for differentiation markers in Figure 4A. **(G)** Lack of rescue of differentiation gene induction loss due to FDXR depletion by enforced MPZL3 expression. Differentiation gene mRNA quantitation in triplicate independent biologic replicates, mean +/- SEM are shown. **(H)** Transcript levels of tagged MPZL3 wild-type, mutant, and truncated proteins used for PLA analysis. **(I)** Immunofluorescence of HA-tagged MPZL3 WT, MPZL3 R99Q, IGV-Like-TM, and TM-LC. Co-localization with MitoTracker is shown. Bar 5 μM.

Supplemental Figure 5. MPZL3 and FDXR Regulate ROS (Related to Figure 5) **(A)** Transcript levels of differentiation markers in the context of MPZL3 and FDXR depletion treated with DMSO control or GAO. n = 3 biological replicates, mean +/- SEM shown. **(B)** Transcript levels of differentiation markers in the context of MPZL3 and FDXR overexpression treated with DMSO control or EUK134. n = 3 biological replicates, mean +/- SEM shown. **(C)**

GSEA of MPZL3 and FDXR KD RNA-Sequencing datasets with NOTCH transcriptional target genes. **(D)** Relative mRNA expression of selected NOTCH transcriptional target genes with siMPZL3 + siFDXR. n = 4 biological replicates, mean +/- SEM shown. **(E)** Quantitative PCR of differentiation markers of differentiated keratinocytes exogenously expressing SOD1 and SOD2. **(F)** Quantification of ROS in cells expressing SOD1 and SOD2. **(G)** Quantitative PCR of differentiation markers in differentiated keratinocytes treated with variable amounts of EUK134. **(H)** Quantification of levels of ROS in differentiated keratinocytes treated with EUK134. **(I)** Quantitative PCR of differentiation markers in differentiated keratinocytes treated with GAO with varied amounts of galactose. **(J)** Quantification of levels of ROS in differentiated keratinocytes treated with GAO.

Supplemental Figure 6. FDXR Enzymatic Activity in Differentiation (Related to Figure 6) **(A)** The reaction catalyzed by FDXR is represented. **(B)** Expression levels in the NADPH rescue experiments in Fig. 6A. **(C)** NADPH levels in the context of MPZL3 depletion. **(D)** ROS levels in the context of FDXR forced expression and depletion of MPZL3 or FDXR. [*] indicates $p < 0.05$, [**] indicates $p < 0.01$. n = 5 biological replicates, mean +/- SEM is shown. **(E)** Standard curve of NADPH assay to demonstrate sensitivity. **(F)** Quantitative PCR of differentiation markers from undifferentiated keratinocytes exogenously expressing an empty vector (EV) control or NOX5. **(G)** Quantitation of NADPH in cells expressing EV or NOX5. **(H)** Quantitation of ROS in cells expressing EV or NOX5. **(H)** PLA of FDXR mutant samples and MPZL3. n=3 biological replicates with at least 10 images analyzed per replicate, mean +/- SEM is shown. Bar 10 μM. **(I)** Quantification of the PLA from (D). **(J)** Expression levels in the rescue experiment in Fig. 6D. **(K)** Bar graph detailing FDXR rescue in the context of MPZL3 depletion. Mean +/- SD shown.

SUPPLEMENTAL TABLE LEGENDS

Supplemental Table 1. (Related to Figure 1) Complete network file for *S. cerevisiae* network. Indicates both nodes of an edge as well as the probability of inclusion in the network.

Supplemental Table 2. (Related to Figure 2) Complete network file for epidermal differentiation network. Indicates both nodes of an edge as well as the probability of inclusion in the network.

Supplemental Table 3. (Related to Figure 3) Dynamic hub scores for most connected nodes from proximity analysis.

Supplemental Table 4. (Related to Figure 2) MPZL3 regulated genes with fold change values.

Supplemental Table 5. (Related to Figure 3) Relative levels of metabolites from differentiated keratinocytes treated with either control siRNA or siRNAs against MPZL3.

Supplemental Table 6. (Related to Figure 4) FDXR regulated genes with fold change values.

EXTENDED EXPERIMENTAL PROCEDURES

Gene Transfer and Knock-down

Transfections of 293T were performed with 10µg lentiviral expression construct, 6µg pCMVΔ8.91, and 2µg pUC MD.G. Transfections were done in 10cm plates using Lipofectamine 2000 (Life Technologies). Viral supernatant was collected at 48 and 72 hours after transfection and concentrated using Lenti-X Concentrator (Clontech). Keratinocytes were transduced overnight with virus and 5µg/ml polybrene, and selected with 1µg/ml puromycin. For siRNA knockdowns, 1 million keratinocytes were electroporated with 1nmol siRNA using Amaxa nucleofection reagents. pLEX vector (Thermo) was the construct used for all lentiviral expression.

cDNA synthesis and qPCR

cDNA was synthesized from total RNA (DNA-free, Qiagen) using the iScript cDNA synthesis kit (Bio-Rad). Quantitative PCR (qPCR) was performed with the Maxima SYBR Green qPCR master mix (Fermentas) on the LightCycler 480 (Roche). Relative mRNA expression was calculated based upon normalization to L32.

BirA* and Mass Spectrometry

A pLEX construct expressing V5-tagged BirA* was generated to express either BirA* alone or as a C-terminal fusion with MPZL3. Undifferentiated keratinocytes were transfected with either the control BirA* vector or the MPZL3-BirA* fusion vector and selected. Per condition, 100 million cells were seeded to differentiation conditions and cultured with biotin. Cell pellets were fractionated to remove cytoplasmic material by resuspending in a swelling buffer (10mM Hepes pH 7.9, 1.5mM MgCl2, 10mM KCl) and lysing with an equal volume of the same buffer plus 0.4% NP-40. After a 1 minute spin at 1500xg, the cytoplasm was removed and the remaining pellet was washed twice with the original swelling buffer. The rest of the purification followed the protocol as previously described (Roux et al., 2012). Material for mass spectrometry was fractionated with a 4-12% SDS-PAGE gel and stained with colloidal blue (Life Technologies), cut into 9 size fractions, and analyzed by the Harvard Mass Spectrometry Facility by microcapillary reverse-phase HPLC nano-electrospray tandem mass spectrometry (µLC/MS/MS) on a Thermo LTQ-Orbitrap mass spectrometer.

Transmission Electron Microscopy

Cells were grown on Aclar then fixed: 0.1% Glutaraldehyde (EMS Cat# 16000) and 4% para-formaldehyde (EMS Cat# 15700) in 0.1M Sodium Cacodylate (EMS Cat# 12300) pH 7.4 for 1 hr at Room Temperature (RT) then washed 3X with ultra-filtered water. Samples were then dehydrated in a series of ethanol washes for 15 minutes each @ 4oC beginning at 30%, 50%, 70%, 95%. Samples are infiltrated with Medium Grade LR White resin (SPI Cat# 02646-AB) mixed 1:1 with 95% EtOH for 1 hr followed by 2 parts LR White resin to 1 part 95% EtOH for 1 hour to overnight then changed 2 X in LR White resin. The samples are then placed into molds w/labels and fresh resin, orientated and placed into 50o C heat block overnight. Sections were taken between 75 and 90nm, picked up on formvar/Carbon coated 100 mesh Ni grids, Immuno-labeled, then contrast stained for 30seconds in 3.5% UrAcetate in 50% Acetone followed by staining in 0.2% Lead Citrate for 3 to 4 minutes. Observed in the JEOL JEM-1400 120kV and photos were taken using a Gatan Orius 4k X 4k digital camera.

Immunoprecipitation

Immunoprecipitation was performed upon differentiated keratinocyte cell pellets fixed for 10 minutes with 1% formaldehyde and lysed with modified RIPA buffer (PBS with 1% NP-40, 0.5% Sodium Deoxycholate, 0.1% SDS, 1mM EDTA). 2µg antibody was added to 1mg lysate for 4 hours. 20ul Protein G beads were added for 1 hour. Beads were washed 4 times in wash buffer (50mM Tris pH 7.5, 5% glycerol, .05% Igepal, 150mM NaCl), and protein was eluted off beads by boiling in LDS sample buffer.

Mitochondrial/Cytoplasmic/Nuclear Fractionation

All steps were performed at 4°C. Fractionation was performed in differentiated keratinocyte cell pellets by resuspension in a swelling buffer (10mM Hepes pH 7.9, 1.5mM MgCl2, 10mM KCl) and lysing was performed in an equal volume of buffer (10mM Hepes pH 7.9, 1.5mM MgCl2, 10mM KCl, 210 mM mannitol, 70 mM sucrose). After a 1 minute spin at 1500xg, the cytoplasm with mitochondria was removed. This fraction was spun at 10,000xg for 15 minutes to pellet the mitochondria. Mitochondrial and nuclear pellets were subsequently lysed in modified RIPA buffer.

Immunofluorescence and Proximity Ligation Analysis (PLA)

Tissue sections were sectioned into 7 micron sections and fixed with either methanol or acetone at -20°C for 10 minutes, and then proceeded to blocking. Keratinocytes were fixed with 4% paraformaldehyde for 5 min followed by 3 PBS washes and permeabilized in PBS with 1%

Triton and 0.1% saponin for 1 hour. Blocking was performed in PBS with 5% bovine serum albumin and 0.1% Triton X-100 for 30 minutes. Primary antibodies were added for 2 hours at room temperature. Standard immunofluorescence proceeded with species specific fluorescently conjugated secondary antibody (Life Technologies) at room temperature for 45 minutes followed by Hoechst staining to mark nuclei for 10 minutes and coverslip fixation with Prolong Gold (Life Technologies). Proximity ligation assay was performed using Duolink with PLA probe anti-mouse plus and PLA probe anti-rabbit minus (Olink Bioscience).

ROS and NADPH Experiments

ROS was detected with DCF-DA (Sigma) by incubating cells with 50 uM DCF-DA for 1 hour at 37°C followed by fluorescent detection at Ex485/Em535. GAO and EUK134 were used as previously described (Hamanaka et al., 2013). NADPH detection was performed using a kit (Abcam) and measuring fluorescence at Ex540/Em590.

Antibodies

MPZL3 antibody was generated by immunizing rabbits with a fusion of the MPZL3 low-complexity region (180-235) with the GST tag. The serum was purified using NHS-activated agarose (Pierce) following manufacturer's instructions. Other antibodies used in this work include: anti-FDXR (Sigma, Ms), anti-Keratin 1 (Covance, Rb), anti-Keratin 10 (Neomarkers, Rb), anti-Loricrin (Covance, Rb), anti-transglutaminase 1 (Biomedical Technology, Ms), anti-HA tag (Covance, Ms; Cell Signaling, Rb), anti-lamin A/C (Cell Signaling, Ms), anti-mitofilin (Life Technologies, Ms) and anti-gamma tubulin (Sigma, Ms). MitoTracker (LifeTechnologies) was incubated at 20 uM with cells for 10 minutes at 37°C prior to normal immunofluorescence protocol.

siRNA Sequences

siRNAs for ZNF750, KLF4, and RCOR1 used were as previously described (Boxer et al., 2014). siRNA used for p63 was as previously described (Sen et al., 2012). siRNAs for MPZL3 were custom designed with Dharmacon and sequences are as follows: siRNA 1:GGACAAUCCUGGAGAUCAU and siRNA 2: GCUAAAGCCUGUCAGAGAA. For FDXR ON-TARGETplus siRNAs (J-008128-06 and J-008128-09) were used (Dharmacon).

Quantitative PCR Primers:

The following primers were used for quantitative PCR:

Gene	Forward Primer	Reverse Primer
L32	AGGCATTGACAACAGGGTTC	GTTGCACATCAGCAGCACTT
MPZL3	CGTCTTTTCCTTGGAGATTCGTG	TTGATACTGTGTGGCTGCTGCTGG
FDXR	AGAAACAGCCTGTGCCCTTT	GAATGGGCCGTCTGGGTAAA
K1	GAAGTCTCGAGAAAGGGAGCA	ATGGGTTCTAGTGGAGGTATCTA
K10	GCAAATTGAGAGCCTGACTG	CAGTGGACACATTTCGAAGG
LOR	CTCTGTCTGCGGCTACTCTG	CACGAGGTCTGAGTGACCTG
FLG	AAAGAGCTGAAGGAACTTCTGG	AACCATATCTGGGTCATCTGG
SPRR3	CCAGGCTACACAAAGCTAC	GCTTAATTCAGGGGCTTAC
TGM1	CTTCAAGAACCCCCTTCCCG	TGAGGATCTTGGGCCTCTGT
TP63	GAGTTCTGTTATCTTCTTAG	TGTTCTGCGCGTGGTCTG
ZNF750	AGCTCGCCTGAGTGTGAC	TGCAGACTCTGGCCTGTA
KLF4	GCCTCCTCTTCGTCGTC	GGCTCACGTCGTTGATGT
RCOR1	AGCAGCTTCTCGCCGTACA	GGTTACTGGGCCCATTGGTCT
MPZL3 -12kb	TGGGTGACTGGGCAAATTGT	TCATCCTCCCAAAGTGCTGG
Gene desert	AAGAGGCCCTTCCTCTATGC	TGTGATTAATCTCGACTCCAAGA

SUPPLEMENTAL REFERENCES

Boxer, L.D., Barajas, B., Tao, S., Zhang, J., and Khavari, P.A. (2014). ZNF750 interacts with KLF4 and RCOR1, KDM1A, and CTBP1/2 chromatin regulators to repress epidermal progenitor genes and induce differentiation genes. Genes & development *28*, 2013-2026.

Feizi, S., Marbach, D., Medard, M., and Kellis, M. (2013). Network deconvolution as a general method to distinguish direct dependencies in networks. Nature biotechnology *31*, 726-733.

Hamanaka, R.B., Glasauer, A., Hoover, P., Yang, S., Blatt, H., Mullen, A.R., Getsios, S., Gottardi, C.J., DeBerardinis, R.J., Lavker, R.M.*, et al.* (2013). Mitochondrial reactive oxygen species promote epidermal differentiation and hair follicle development. Science signaling *6*, ra8.

Kretz, M., Webster, D.E., Flockhart, R.J., Lee, C.S., Zehnder, A., Lopez-Pajares, V., Qu, K., Zheng, G.X., Chow, J., Kim, G.E.*, et al.* (2012). Suppression of progenitor differentiation requires the long noncoding RNA ANCR. Genes & development *26*, 338-343.

Marbach, D., Costello, J.C., Kuffner, R., Vega, N.M., Prill, R.J., Camacho, D.M., Allison, K.R., Consortium, D., Kellis, M., Collins, J.J.*, et al.* (2012). Wisdom of crowds for robust gene network inference. Nature methods *9*, 796-804.

Roux, K.J., Kim, D.I., Raida, M., and Burke, B. (2012). A promiscuous biotin ligase fusion protein identifies proximal and interacting proteins in mammalian cells. The Journal of cell biology *196*, 801-810.

Sen, G.L., Boxer, L.D., Webster, D.E., Bussat, R.T., Qu, K., Zarnegar, B.J., Johnston, D., Siprashvili, Z., and Khavari, P.A. (2012). ZNF750 is a p63 target gene that induces KLF4 to drive terminal epidermal differentiation. Developmental cell *22*, 669-677.